Weak molecular chemisorption of N_2/Pt(111)

2009 J. Phys.: Condens. Matter 21 264009

(http://iopscience.iop.org/0953-8984/21/26/264009)

J. Phys.: Condens. Matter **21** (2009) 264009 (7pp) doi:10.1088/0953-8984/21/26/264009

Weak molecular chemisorption of N_2/Pt(111)

L W Bruch[1], R P Nabar[2] and M Mavrikakis[2]

[1] Department of Physics, University of Wisconsin-Madison, 1150 University Avenue, Madison, WI 53706, USA
[2] Department of Chemical and Biological Engineering, University of Wisconsin-Madison, 1415 Engineering Drive, Madison, WI 53706, USA

Received 24 October 2008, in final form 26 November 2008
Published 11 June 2009
Online at stacks.iop.org/JPhysCM/21/264009

Abstract
The ordering in a higher-order-commensurate monolayer solid of Pt(111)-(3 × 3)-4 N_2, which has coexisting physisorbed and weakly chemisorbed N_2 species, is analyzed with model calculations. Density functional theory calculations are also used to evaluate properties of chemisorbed N_2 in a (2 × 2) unit cell on Pt(111). The relation of these results to the orientational ordering of N_2 on other metal surfaces is discussed.

(Some figures in this article are in colour only in the electronic version)

1. Introduction

A quite satisfactory quantitative understanding of a great range of observations has been achieved [1] for inert gas monolayers. However, monolayers of physically adsorbed linear molecules already present a much greater variety of phenomena and the understanding is more qualitative. Observations of orientational ordering in monolayer solids of molecular nitrogen N_2 on the basal plane surface of graphite [2, 3] are reproduced by model calculations, but the evidence for orientational ordering for N_2 on metals is mostly indirect and more limited in conclusiveness.

Many reports of structural experiments for physisorbed layers of N_2 molecules on metal surfaces are accompanied by model calculations. Almost all of the calculations are based on N_2–substrate potential energies formed by atom–atom potential sums, although it is likely that a realistic theory of physical adsorption on metals will require some level of quantum chemistry. The metal substrates for which atom sum constructions are done include Cu(110) [4], Ag(111) [5], Ag(110) [6], and Pt(111) [7]. Some features of experimental adsorption energies are reproduced, but the relative stability of molecular orderings, the placement of the monolayer solid lattice relative to the substrate, and the corrugation of the adsorbing surface are still in question.

In this context, observations on the monolayer solid of Pt(111)-(3 × 3)-4 N_2 are of great interest. The initial helium atom scattering data [7] were modeled using analogies to physical adsorption on graphite and assigned to a herringbone lattice. More recent experiments [8] using infrared absorption demonstrate that there are coexisting physisorbed and weakly chemisorbed N_2 molecules in this solid, probably in a four-sublattice pinwheel with the vertical molecule atop a surface platinum atom, as in figure 1. This placement and the stability of the pinwheel relative to the herringbone lattice are features that are difficult to reproduce with pair-wise sums for the holding potential. Here we present a stability analysis to make some estimates of the N_2–Pt(111) potential energy surface and calculations with density functional theory to confirm that the observed intramolecular vibration frequency and adsorption-induced dipole moment of the N_2 can be reproduced by electronic structure theory.

Experiments on mechanisms of friction at the nanoscale provide an additional stimulus for improving the basic understanding of the monolayers of linear molecules. Sliding friction of monolayers on metals is expected to have dissipation channels involving excitation of both phonon and electron degrees of freedom of the metals. Krim and co-workers [9] demonstrated the presence of the electron dissipation channel in the slippage of monolayers on Pb(111). In their quartz crystal microbalance (QCM) experiments, there was a discontinuous change in the damping as the temperature was reduced below the superconducting transition of lead at 7.2 K. The effect was observed only for N_2 and not for the inert gases Ne and Xe. The 7.2 K temperature is well below the estimated [5] orientational ordering of monolayer N_2. It was proposed [10] that the effect for N_2/Pb(111) is related to electric fields arising from an ordered herringbone array of electrostatic quadrupoles. While monolayer orientational ordering is expected at low temperatures, there is much

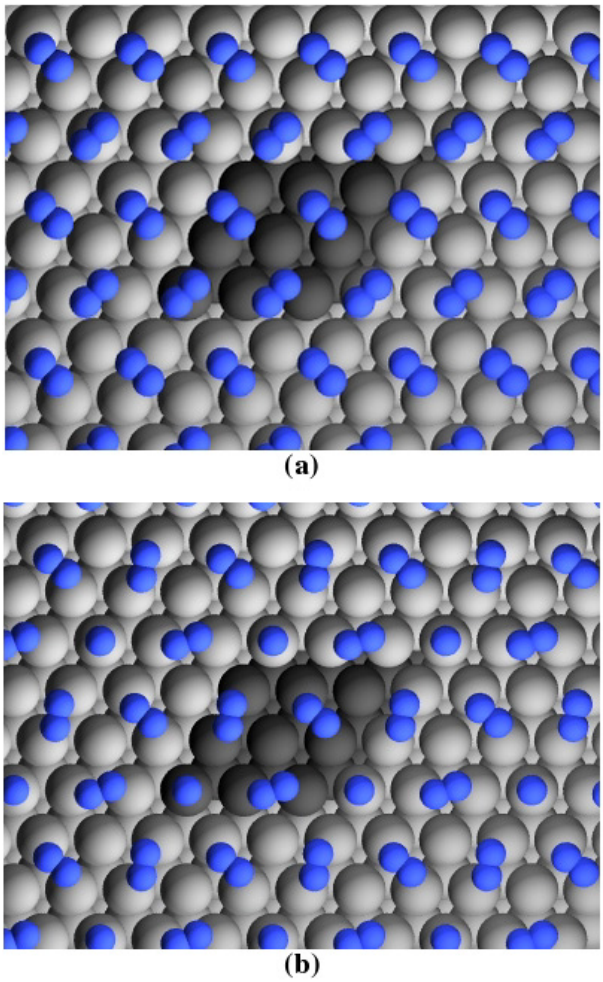

Figure 1. Schematic diagrams for the herringbone and pinwheel lattices of Pt(111)-(3 × 3)-4 N_2. The large spheres are platinum atoms and the 3 × 3 unit cell is highlighted as darker spheres. The diatomics are N_2 molecules arranged in (a) a 2-in herringbone and (b) a four-sublattice pinwheel with the 'pin' molecule placed erect atop a platinum atom.

uncertainty (experimental and theoretical) in the nature of the ordering on single crystal metal surfaces. In particular, although 2-in herringbone ordering is predicted for one of the N_2/Pt(111) lattices [7] and for N_2/Ag(111) [5], there is no direct experimental confirmation for those cases or for N_2/Pb(111). That leaves a concern that the predictions may be artifacts of the holding potential models.

The organization of this paper is as follows: section 2 contains a brief review of experiments on N_2/Pt(111); section 3 presents an analysis using pair-potential models; section 4 presents the results of density functional calculations. Conclusions are given in section 5 and there is an appendix summarizing evidence for orientational ordering in other N_2 monolayers.

2. Review of data for N_2/Pt(111)

This has the most extensive data set of any example of N_2 physically adsorbed on a metal.

There are helium atom scattering (HAS) diffraction peaks showing [7] (3 × 3) and (4 × 4) unit cells of N_2/Pt(111). In that experiment the (3 × 3) unit cell transformed into the (4 × 4) under annealing at 40 K and then was stable with cooling to 20 K. The monolayer heat of adsorption is rather large, $q_1 = 158 \pm 5$ meV, and the 2D latent heat of condensation is $q_{2D} = 21 \pm 3$ meV. The diffraction pattern for the (3 × 3) lattice has a weak peak at (1/3, 0) and a strong one at (2/3, 0); assigning the latter to the average N_2 lattice (four molecules in the unit cell) gives a nearest-neighbor spacing $L_{nn} = 4.155$ Å and area per molecule $A = 14.95$ Å^2. Modeling suggests [7] that there are seven molecules in the (4 × 4) cell, which can be arranged in a triangular average center-of-mass lattice with $L_{nn} = 4.188$ Å and $A = 15.19$ Å^2.

Another set of experiments [11] that included temperature programmed desorption (TPD) and reflection–absorption infrared spectroscopy (RAIRS) gave a desorption energy of 150 meV, agreeing with q_1, and an intramolecular stretching frequency of 2266 cm^{-1} (=281 meV), shifted by 65 cm^{-1} (=8 meV) from the gas phase value of 2331 cm^{-1} (=289 meV). Another absorption at 2222 cm^{-1} (=276 meV) was assigned to N_2 chemisorbed at surface defects. There was no diffraction determination of the adsorbed N_2 structure.

Gustafsson and Andersson [8, 12] extended the RAIRS measurements and augmented them with low energy electron diffraction (LEED) and work function measurements. A work function change of −0.13 eV was modeled as an adsorption-induced dipole moment of 0.06 D on the N_2. They reported, but did not show, LEED observations that N_2/Pt(111) adsorbs at 30 K in a (3 × 3) commensurate monolayer (consistent with Zeppenfeld *et al* [7], in the absence of annealing). Most striking, there was an N_2 stretching frequency of 2322 cm^{-1} as well as the 2266 cm^{-1} frequency previously found [11]. Analysis of the growth of the integrated absorbances with exposure and the absolute values led to an identification of the (3 × 3) unit cell as having four molecules, three of them scarcely perturbed and one with a 65 cm^{-1} shift in intramolecular vibration frequency. Electronic energy calculations [13, 14] were cited in support of the assignment of the perturbed N_2 molecule as 'weakly chemisorbed' and arranged perpendicular atop a surface platinum atom. The likely structure, (meta)stable at 30 K, is a classic pinwheel with four molecules in the unit cell.

Some of these features for N_2/Pt(111) parallel data [15] for N_2/Pd(111), where N–N excitations at 289 and 280 meV are observed for the monolayer. However, both 'species' desorb at 45 K for N_2/Pt(111) but they desorb at 61 and 72 K, respectively, for N_2/Pd(111). Also, the work function change of approximately −0.6 eV for monolayer N_2/Pd(111) is much larger than the −0.1 eV for N_2/Pt(111).

The quantum of perpendicular (z) vibrations measured by inelastic helium atom scattering for physisorbed N_2 in the (4 × 4) higher-order-commensurate (HOC) lattice is [7] $\hbar\omega_\perp = 5.0$–5.2 meV. For comparison, the molecule–substrate vibration frequency $\tilde{\nu}$ and the intramolecular stretch ν(N–N) of weakly chemisorbed molecular N_2 are $\tilde{\nu} = 26$ meV and ν(N–N) = 280 meV for N_2/Pd(111) [15], and $\tilde{\nu} = 35$ meV and ν(N–N) = 272 meV for N_2/Ru(0001) [16].

Table 1. Components of the lateral potential energy for four N_2/Pt(111) monolayer solids. The 2-in herringbone (HB), 4-molecule pinwheel (PW) and perpendicular aligned (3 ⊥) have centers of mass on a triangular lattice with $L_{nn} = 4.155$ Å, while the $(\sqrt{3} \times \sqrt{3})$R30° lattice ($\sqrt{3}$) has N_2 perpendicular to the surface and $L_{nn} = 4.80$ Å. Interactions as described in section 3. The center-of-mass heights are determined by the $V_0(z)$ of the N_2–Pt(111) model. E_{LJ} denotes the N_2–N_2 LJ(12, 6) energy, E_Q the quadrupole energy using a distributed point charge model, E_{QI} the corresponding energy arising from the image (screening) charges on the Pt, and E_M the McLachlan substrate-mediated dispersion energy. Energies per molecule in meV.

Energy	HB [a]	PW [b]	3 ⊥ [c]	$\sqrt{3}$[d]
E_{LJ}	−27.2	−29.0	−28.6	−14.4
E_Q	−3.7	−5.5	4.9	2.4
E_{QI}	0.2	−0.1	0.3	0.3
E_M	2.5	2.2	1.8	1.0
Total	−28.2	−32.4	−21.6	−10.7

[a] Four molecules arranged as two 2-in herringbone pairs (see Zeppenfeld *et al* [7]) with 14.95 Å^2/molecule. The corresponding potential energy for a minimum energy 2D 2-in herringbone lattice is [32] $E_{LJ} + E_Q = -31.4$ meV at 14.86 Å^2/molecule.

[b] The 'pin' molecule is perpendicular to the plane and three near-planar 'wheel' molecules are at successive 120° rotations, with the first one at 19 ° to the pinwheel axis. The center of the 'pin' molecule is 0.4 Å higher than that of a 'wheel' molecule. An unsupported 2D layer with the centers of all four molecules in the same plane has $E_{LJ} = -29.2$ meV and $E_Q = -5.7$ meV.

[c] Special case of a three-molecule superlattice proposed by Knorr *et al* [33] for CF_3Br on graphite.

[d] All the N_2 are in the same environment for this simply commensurate lattice.

3. Modeling of physisorbed Pt(111)-(3 × 3)-4 N_2

The interaction model is very similar to that used by Zeppenfeld *et al* [7] for N_2/Pt(111) and by Roosevelt [17] for N_2/graphite. The N_2–N_2 interactions are given by the X1 model of Murthy *et al* [18] supplemented by the McLachlan energy using $C_{s1} = 45.73$ and $C_{s2} = 31.08$ au. The interaction of N_2 with the substrate is constructed from a sum of Lennard-Jones (12, 6) potentials for N–Pt pairs with $\epsilon = 5.8$ meV and $\sigma = 3.82$ Å.

Results for minimum potential energy configurations, after optimizing the molecular orientations and N_2–Pt(111) heights, are presented in tables 1 and 2. Table 1 shows components of the molecule–molecule potential energy for four monolayer lattices. The zero point energy of a 2D solid of N_2 at $A = 15.0$ Å^2 is approximately 7.3 meV in the lattice dynamical calculations of Roosevelt [17] for uniaxially incommensurate (UIC) N_2/graphite. Thus the net 2D heat of sublimation calculated for the 2-in herringbone (HB) at 0 K is approximately 21 meV and is close to the experimental 2D heat of value $q_{2D} = 21 \pm 3$ meV of Zeppenfeld *et al* [7]. There do not seem to be major terms missing from the model of the N_2–N_2 interactions.

Table 2. Calculated energies for HB and PW configurations of Pt(111)-(3 × 3)-4 N_2. See section 3 for identification of these entries. The experimental monolayer heat of condensation is [7] $q_1 = 158 \pm 5$ meV. Energies are in meV/molecule.

Term	HB	PW
$E_{LJ} + E_Q$	−30.9	−34.5
E_{lat}	−28.2	−32.4
Φ ('flat')	−162.3	−159.6
Φ (corrugated)	−162.4	−160.3
E_z[a]	12.5	12.5
E_{tot}	−150	−148

[a] Calculations [17] for the UIC N_2/graphite at $A = 15.0$ Å^2 give a zero point energy of 13.5 meV for 3D motions of the monolayer, but $\omega_\perp$ is ≈1 meV larger for N_2/graphite than for N_2/Pt(111). Hence 12.5 meV/molecule is used as an estimate of the zero point energy for N_2/Pt(111)-(3 × 3)-4 N_2. This includes an adjustment for the N_2 libration that is nearly degenerate with $\omega_\perp$.

The total N_2–N_2 potential energies for the four-sublattice pinwheel (PW) and HB cases are −32.4 and −28.2 meV, respectively. That is, the PW configuration is intrinsically a lower energy 2D arrangement at this density and the HB is stabilized by the energy increment to make the 'pin' molecule perpendicular to the plane, as seen from the entries in table 2. The total potential energy including the N_2–'flat' Pt(111) interaction is −159.6 meV for the PW and −162.3 meV for the HB. On the corrugated surface the values are −160.3 and −162.4 meV, respectively. The pin molecule on the corrugated surface is at a threefold hollow. That the HB has lower energy than the PW and the nature of the pin-site are generic features of molecule–substrate potential energy surfaces formed from atom–atom sums. They persist under several modifications of the interaction model.

However, the RAIRS data [8] strongly indicate that the PW lattice is the stable configuration for the (3×3) HOC lattice of N_2/Pt(111). The following argument gives an estimate of the change needed in the N_2–Pt(111) holding potential model to reproduce this conclusion.

Start from the assumption that the N_2–Pt(111) potential has its minimum energy site with N_2 perpendicular and atop a Pt atom, in analogy to Xe/Pt(111) [1], and examine what information about the potential energy surface can be inferred from the requirements that (1) the PW has lower energy than the HB for $L_{nn} = 4.155$ Å and (2) the $\sqrt{3}$ simply commensurate lattice with $L_{nn} = 4.80$ Å and all molecules perpendicular to the surface has higher energy than this PW. Let $V_{0\|}$ be the average holding potential for molecules nearly parallel to the plane and $\Delta V_\perp$ be the increment in energy for a molecule oriented perpendicular to the plane and atop a Pt atom. The total potential energies per molecule, using the values of E_{LJ} and E_Q given in table 1, are

$$E(\mathrm{HB}) = V_{0\|} - 30.9 \text{ meV}, \quad (1)$$

Table 3. Height in Å at atop site. Unless otherwise specified the experimental values Z (direct) (from LEED intensity analyses) and density functional theory values Z (LDA) (local density approximation) and Z (GGA) (generalized gradient approximation) are taken from a recent review [1].

System	Z (vdW) [a]	Z (direct)	Z (LDA)	Z (GGA)
Xe/Pt(111)	3.56	3.40	3.07	3.62
Xe/Pd(111)	3.54	3.07	2.85	3.27
Xe/Cu(111)	3.44	3.60	3.26	4.03
Xe/Ru(0001)	3.52	3.54		
Kr/Pd(111)	3.37		2.94 [b]	3.54 [b]
Kr/Ru(0001)	3.35	3.70 [c]	3.09 [d]	
N_2/Ru(0001)	3.35	2.55 [e]		
N_2/Pt(111)	3.38			2.58 [f]

[a] Sum of van der Waals radii, equal to one-half the nearest-neighbor spacing in the 3D crystal ground states.
[b] From Da Silva and Stampfl [34].
[c] Overlayer height at a threefold hollow site.
[d] At an atop site, calculation of Yang *et al* [36].
[e] Molecular center from Bludau *et al* [35].
[f] Molecular center from this work, section 4. GGA values of Karlberg [8] obtained by fitting Z to ν(N–N) are $Z = 2.78$ Å for ν(N–N) $= 2266$ cm^{-1} (weakly chemisorbed N_2) and $Z = 3.2$ Å for ν(N–N) $= 2331$ cm^{-1} (unperturbed N_2).

$$E(\mathrm{PW}) = V_{0\parallel} + \tfrac{1}{4}\Delta V_\perp - 34.5\ \mathrm{meV}, \tag{2}$$

$$E(\sqrt{3}) = V_{0\parallel} + \Delta V_\perp - 12.0\ \mathrm{meV}. \tag{3}$$

The relative stability conditions give bounds $E(PW) < E(HB) \Rightarrow \Delta V_\perp < 14.4$ meV and $E(PW) < E(\sqrt{3}) \Rightarrow \Delta V_\perp > -30$ meV. Together these set a range

$$-30\ \mathrm{meV} < \Delta V_\perp < 14\ \mathrm{meV}. \tag{4}$$

The upper bound largely comes from differences in the electrostatic (quadrupolar) energies in the structures; it shows that the PW can be stable without the atop site being the minimum potential energy site.

The atom–atom sum model used by Zeppenfeld *et al* [7] has $\Delta V_\perp \approx 26$ meV. This is also the size estimated from the measured quantum of perpendicular vibration of a (parallel) molecule, $\hbar\omega_\perp \simeq 5$ meV, which gives a force constant $K = m_N\omega_\perp^2 = 1.4$ J m^{-2} for N atoms bound to the platinum. Then the energy increment for tipping the ends of the molecule (length ℓ) about its center of mass, $\delta z = (\ell/2)\sin\phi$, is

$$\Delta E = 2 \times \tfrac{1}{2}K(\ell/2)^2\sin^2\phi \simeq 26\sin^2\phi\ (\mathrm{meV}) \tag{5}$$

and the energy to tip from $\parallel$ to $\perp$ is 26 meV. The close agreement of these two values is coincidental because the interaction model has $\hbar\omega_\perp \simeq 7$ meV and the center of the molecule is 0.4 Å higher in the $\perp$ configuration. However, values $\Delta V_\perp > 20$ meV are usually obtained for the pair-potential sum constructions of holding potentials on metals.

The average holding potential obtained by combining the experimental q_1 and q_{2D} is ≈ -135 meV. Then a value $\Delta V_\perp \approx -10$ meV, which would give a stable PW, corresponds to a somewhat more corrugated energy surface than N_2/graphite and less corrugated than Xe/Pt(111) [1]. However, this requires a quite different construction for the N_2–Pt potential, as does atop site adsorption. Another indication of a need for revision of the N_2–Pt potential model [7] is the equilibrium height Z_{eq} of ($\parallel$) N_2 above the surface. The model gives $Z_{eq} \simeq 3.70$ Å, but the height of the molecular center at the top-site calculated using the van der Waals radii of the 3D N_2 and Pt solids is Z(vdW) $\simeq 3.40$ Å and this is probably an overestimate. The calculations described in section 4 give an N–N stretch frequency of 2281 cm^{-1} at a height $Z = 2.56$ Å of the molecular center from the plane of the surface Pt atoms. Comparisons of experimental Z and estimates are shown in table 3.

4. Density functional theory calculations for N_2/Pt(111)

4.1. Computational methods

All calculations are performed using DACAPO [19], a periodic self-consistent DFT-based total-energy code. Adsorption is allowed on only one of the two exposed surfaces, with the electrostatic potential adjusted accordingly [20]. Ionic cores were described by ultrasoft pseudopotentials [21], and the Kohn–Sham one-electron valence states are expanded in a basis of plane waves with kinetic energy below 25 Ryd. The exchange–correlation energy and potential are described self-consistently within the generalized gradient approximation (GGA-PW91) [22]. The self-consistent PW91 density is determined by iterative diagonalization of the Kohn–Sham Hamiltonian, Fermi population of the Kohn–Sham states ($k_BT = 0.1$ eV), and Pulay mixing of the resulting electronic density [23]. All total energies have been extrapolated to $k_BT = 0$ eV. Most of the calculations are with a three-layer metal slab and 2×2 surface unit cell. The top layer is allowed to relax (about 1% expansion relative to the lower layer). Calculations with larger (3×3) surface unit cells and a four-layer slab confirm this inter-layer relaxation is in the 1–2% range. The surface coverage with one adsorbate N_2 molecule per surface 2×2 cell is 1/4 ML. The unit cell is repeated in super-cell geometry with successive slabs separated by a vacuum region equivalent to five metal layers thick. The surface Brillouin zone is sampled at 18 special Chadi–Cohen k-points [24]. The calculated equilibrium PW91 lattice constant for Pt (4.00 Å) is in good agreement with the experimentally determined value of 3.92 Å [25].

Vibrational frequencies are determined by diagonalization of the mass-weighted Hessian matrix; a second-order finite difference approximation (step size 0.01 Å) of the PW-91 calculated force derivatives is used to construct this matrix [26]. The metal atoms are fixed in their relaxed geometries for these calculations; only the adsorbate atoms are displaced from their minimum energy coordinates. This approximation is not expected to introduce significant error into the results and is equivalent to the assumption that the adsorbate and metal modes are essentially decoupled.

4.2. DFT results

The DFT calculations with a self-consistent GGA-PW91 functional give a binding energy (BE) of -0.18 eV for N_2

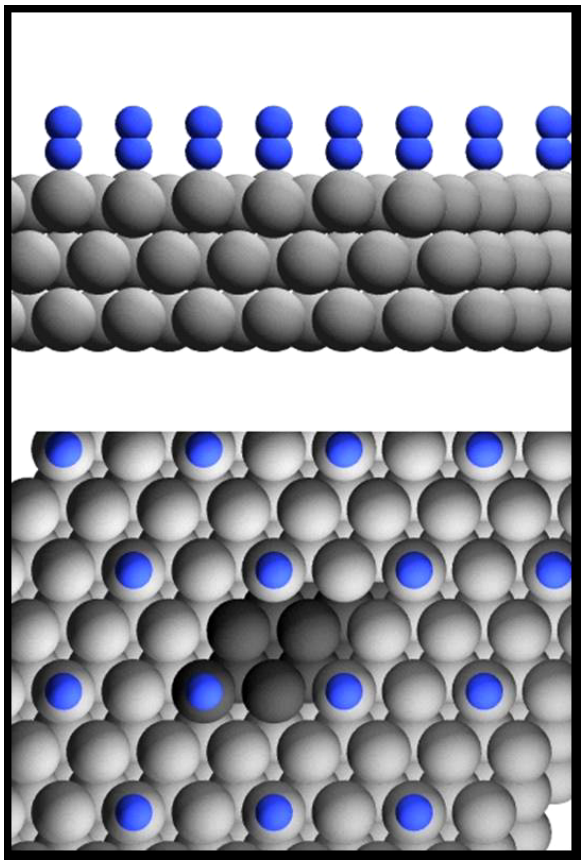

Figure 2. Preferred site for N_2 adsorption on Pt(111)—two perspectives: the top panel gives a cross-section view of the slab, the bottom an on-top view of the slab. The topmost layer of Pt atoms is relaxed from its bulk-truncated position whereas the bottom two layers are static. A single 2×2 unit cell is highlighted in darker gray as a guide to the eye (small/blue = N, large/gray = Pt).

adsorbed 'end-on' at the top-site (figure 2). These calculations are performed at an effective N_2 coverage of $\frac{1}{4}$ ML and the preferred adsorption site is the same as in previous work by Ford *et al* [14] and Tripa *et al* [13]. The geometric details of the adsorbed N_2 state are provided in figure 3. The adsorption of N_2 is perpendicular to the (111) facet. The calculated N–N bond length is 1.13 Å and the bottom N atom is 1.99 Å above the Pt atom that is immediately below it. The 2×2 unit cell has four Pt atoms and the Pt atom that is bonded to and immediately below the N_2 molecule is raised slightly from its equilibrium position. This offset of 0.19 Å is also shown in figure 3. The other three Pt atoms in the surface unit cell are depressed very slightly from their original position and thus the major effect of the nitrogen molecule seems to be on the Pt atom directly below it. This was also found in the calculations for the 3×3 unit cell and the four-layer slab.

Adsorption of N_2 was also investigated for other high-symmetry sites on the Pt(111) surface including the fcc, hcp and bridge sites. Exothermicity of N_2 adsorption on these sites at $\frac{1}{4}$ ML coverage is marginal. All these cases have very weak binding ($|BE| < 0.04$ eV) and the molecule is located much further away from the Pt surface and is oriented perpendicular or in a tilted configuration. The vertical separation between

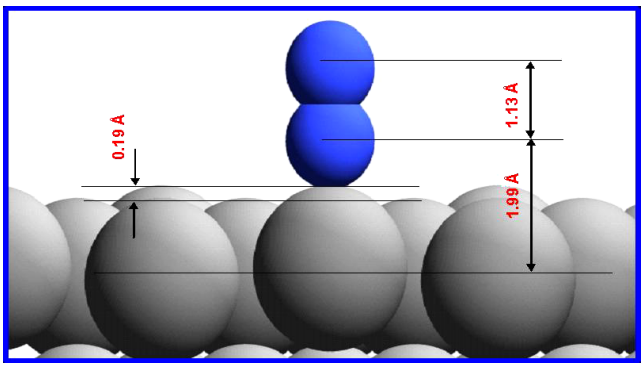

Figure 3. Geometrical parameters for N_2 adsorption at an atop site on Pt(111). (small/blue = N, large/gray = Pt).

the Pt surface and the closer-to-the-surface N atom for the fcc, hcp and bridge sites is 3.59, 3.10 and 3.70 Å, respectively. Thus, these weakly bound physisorbed configurations are further away from the surface than the chemisorbed atop site (vertical separation of 1.99 Å; see figure 3). We note that our calculations do not include van der Waals interactions, which may be dominant for weak binding.

The calculations also give estimates of the dipole moment at each of the adsorption sites: the close-to-surface vertically adsorbed N_2 molecule at the atop site has the strongest dipole moment (0.35 D) whereas the other three configurations (corresponding to physisorbed molecules further away from the surface) have much lower dipole moments (<0.1 D). Then the dipole moment per molecule averaged over the four molecules in the PW structure for Pt(111)-(3×3)-4 N_2 would have magnitude smaller than 0.16 D and on the scale of the 0.06 D inferred from work function measurements [8].

The vibrational modes and frequencies were evaluated for each of the adsorption states. For N_2 adsorbed at the atop site, two modes were obtained: (a) N–N stretch at 2281 cm^{-1} and (b) N–Pt stretch at 296 cm^{-1}. This value for the N–N stretch frequency is in close agreement with the experimental results of Gustafsson *et al* [8] for the chemisorbed N_2 state. Vibrational frequencies were also obtained for the other weakly bound N_2 sites with the molecule further from the Pt(111) surface and for an isolated (gas phase) N_2 molecule. The N–N stretch mode is again the dominant mode and the frequencies are very similar for all the weakly bound states (figure 4) but significantly different than for the strongly adsorbed N_2 at the atop site. A comparison of the vibrational frequencies for these sites with that for gas phase N_2 shows that the physisorbed states have frequencies very similar to the gas phase N_2 molecule, whereas the atop chemisorbed site has a downshifted frequency (figure 4).

Since stable chemisorption was not obtained at any of the other sites it is difficult to determine the diffusion barrier for N_2 on Pt(111). The difference in the calculated binding energy at the atop site (−0.18 eV) and the physisorbed states (ca. −0.04 eV) gives an estimate of ca. 0.14 eV for the surface diffusion barrier. However, this estimate is not very informative in light of the observed surface mobility of N_2 at 35–40 K, which already indicates the barrier should be much lower.

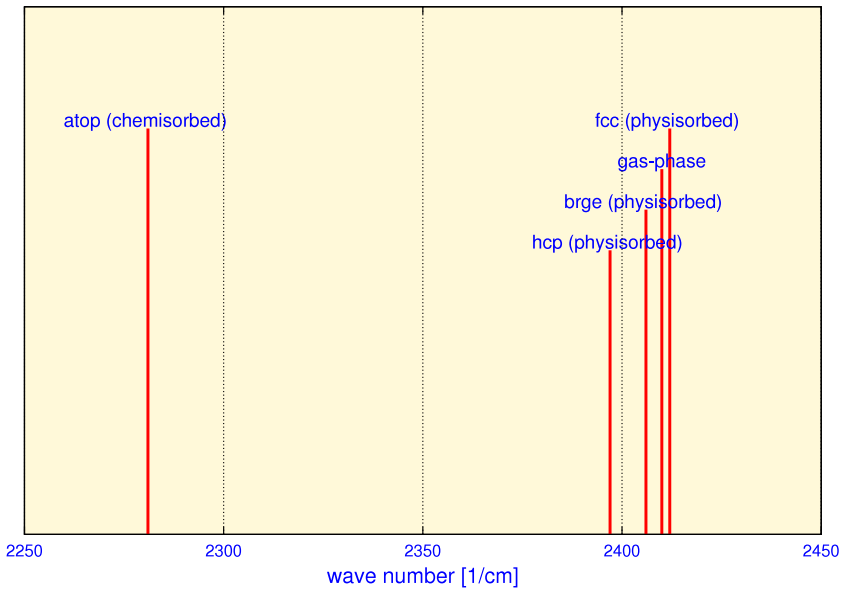

Figure 4. Comparison of the N–N stretch frequencies in cm^{-1} (1 cm^{-1} = 0.124 meV) for chemisorbed N_2, physisorbed N_2 and gas phase N_2. The heights of the bars are varied only to help distinguish the frequencies.

The energy quantum corresponding to the N_2–Pt(111) stretch frequency of 296 cm^{-1} is 36.7 meV. This is in the range of the molecule–surface vibration quantum for weakly chemisorbed N_2 on Pd(111) and Ru(001) [15, 16], but it is outside the range of energies accessible in the inelastic HAS experiment [7] for N_2/Pt(111). The DFT calculation shows that the N_2 molecule vibrates as a molecular unit in a direction along the axis perpendicular to the Pt(111) facet with almost no change in the N–N bond length during the vibration.

5. Concluding remarks

If the conventional atom–atom sum method for generating N_2–metal potential energy surfaces is suspect, especially for configurations involving the tilt of molecular axes out of the monolayer plane, the orientational order in the physical monolayer solid may be more complex than that of the (2-in) planar herringbone. However, it is not evident than this should strongly decrease the ordering temperature from the ≈28 K observed for N_2/graphite. The RAIRS experiments on (3×3) commensurate N_2/Pt(111) strongly support the existence of (non-planar) orientational order in that system at 30 K. The DFT calculations suggest that that an N_2–Pt stretch mode at about 300 cm^{-1} should be sought in future RAIRS experiments on this system.

Acknowledgments

It is a pleasure to thank Professor R D Diehl for many conversations about the adsorption of nitrogen on metals and Professor J M Phillips for a preprint of his calculations on Kr/Ru(0001). Work done by RN and MM has been supported by US-DoE-NETL grant DE-FC26-03NT41966. Supercomputing time at ANL, PNNL, ORNL and NERSC resources is gratefully acknowledged

Appendix. Orientational order in other N_2 monolayer solids

N_2 adsorbed on graphite is the most extensively studied molecular physisorption system [2]. The interaction model for N_2 with the graphite substrate is constructed as an atom–atom sum, in analogy to the constructions for inert gases on graphite. The monolayer heat of adsorption is $q_1 = 110 \pm 9$ meV. The orientationally ordered state of commensurate N_2/graphite (area per molecule $A = 15.72$ $Å^2$) was shown to be a planar herringbone array (‘2-in’) by observation of a diffraction pattern with two glide plane symmetries and superlattice diffraction peaks. The ordering temperature is 28 K and is nearly that in the uniaxially incommensurate (UIC) lattice. Simulations with several interaction models [27–29] give an ordering temperature in the range 33–22 K.

LEED measurements of Leatherman and Diehl [30] for the monolayer solid of N_2/Ag(111) covered the temperature range 25–42 K without any sign of an orientationally ordered solid. The nearest-neighbor spacings of molecular centers in the compressed triangular monolayer lattice, 4.00–4.15 Å, are in a range that had been observed for compressed triangular incommensurate monolayer solids of N_2/graphite. The derived monolayer compressibility is comparable [5] to that calculated for incommensurate N_2/graphite. The monolayer heat of condensation is $q_1 = 103 \pm 4$ meV and the compressed solid has $A = 13.9$–14.9 $Å^2$. The predicted orientational ordering temperature for a 2-in herringbone lattice is [5] ≈20 K, using a model similar to one that gave [29] 22 K for commensurate N_2/graphite. High-resolution electron-energy-loss spectroscopy (HREELS) for N_2/Ag(111) gave [31] ν(N–N) = 289 meV, the gas phase value, which is further support for an assignment as physisorption.

A higher-order-commensurate (HOC) lattice of N_2/Cu(110), observed by HAS measurements [4] in the

temperature range 20–32 K, was identified, on the basis of model calculations, as a unit cell with seven molecules in a pinwheel structure and $A = 14.45$ Å^2. No abrupt order–disorder transition was observed and there were no extinctions of any of the main diffraction spots of the superlattice. The calculated packing energies of several candidate unit cells strongly suggested an arrangement of six nearly planar ($\parallel$) and one vertical ($\perp$) molecule [4]. The monolayer heat of condensation is $q_1 = 88 \pm 4$ meV and the 2D heat of condensation is $q_{2D} = 5.5 \pm 0.5$ meV.

LEED and TPD experiments [6] showed that a monolayer solid of N_2/Ag(110) is formed with $A = 15.7$ Å^2 and $q_1 = 104 \pm 1$ meV, values that are similar to those for the triangular incommensurate lattices of N_2/Ag(111). The diffraction was performed at $T = 15$ K and only the leading average-lattice diffraction peaks were observed because of experimental constraints. That is, there is no direct experimental evidence for the existence and character of orientational ordering in N_2/Ag(110) at 15 K. Model calculations suggested that the monolayer has a herringbone HOC lattice.

References

[1] Bruch L W, Diehl R D and Venables J A 2007 *Rev. Mod. Phys.* **79** 1381
[2] Marx D and Wiechert H 1996 *Adv. Chem. Phys.* **95** 213
[3] Diehl R D and Fain S C Jr 1983 *Surf. Sci.* **125** 116
[4] Marmier A, Ramseyer C, Girardet C, Goerge J, Zeppenfeld P, Büchel M, David R and Comsa G 1997 *Surf. Sci.* **383** 321
Zeppenfeld P, Goerge J, Diercks V, Halmer R, David R, Comsa G, Marmier A, Ramseyer C and Girardet C 1997 *Phys. Rev. Lett.* **78** 1504
[5] Bruch L W and Hansen F Y 1998 *Phys. Rev.* B **57** 9285
[6] Ramseyer C, Girardet C, Bartolucci F, Schmitz G, Franchy R, Teillet-Billy D and Gauyacq J P 1998 *Phys. Rev.* B **58** 4111
Teillet-Billy D, Gauyacq J P, Bartolucci F, Franchy R, Ramseyer C and Girardet C 2000 *Surf. Sci.* **465** 138
[7] Zeppenfeld P, David R, Ramseyer C, Hoang P N M and Girardet C 2000 *Surf. Sci.* **444** 163
[8] Gustafsson K, Karlberg G S and Andersson S 2007 *J. Chem. Phys.* **127** 194708
[9] Dayo A, Alnasrallah W and Krim J 1998 *Phys. Rev. Lett.* **80** 1690
Krim J 2007 *Nanotoday* **2** 38
[10] Bruch L W 2000 *Phys. Rev.* B **61** 16 201
[11] Zehr R, Solodukhin A, Haynie B C, French C and Harrrison I 2000 *J. Phys. Chem.* B **104** 3094
[12] Gustafsson K and Andersson S 2006 *J. Chem. Phys.* **125** 044717
[13] Tripa C E, Zubkov T S, Yates J T Jr, Mavrikakis M and Nørskov J K 1999 *J. Chem. Phys.* **111** 8651
[14] Ford D C, Xu Y and Mavrikakis M 2005 *Surf. Sci.* **587** 159
[15] Bertolo M and Jacobi K 1992 *Surf. Sci.* **265** 1
Bertolo M and Jacobi K 1992 *Surf. Sci.* **265** 12
[16] Shi H and Jacobi K 1992 *Surf. Sci.* **278** 281
[17] Roosevelt S E and Bruch L W 1990 *Phys. Rev.* B **41** 12236
Roosevelt S E 1989 *PhD Thesis* University of Wisconsin-Madison (unpublished)
[18] Murthy C S, Singer K, Klein M L and McDonald I R 1980 *Mol. Phys.* **41** 1387
[19] Greeley J, Nørskov J K and Mavrikakis M 2002 *Annu. Rev. Phys. Chem.* **53** 319
Hammer B, Hansen L B and Nørskov J K 1999 *Phys. Rev.* B **59** 7413
[20] Neugebauer J and Scheffler M 1992 *Phys. Rev.* B **46** 16067
Bengtsson L 1999 *Phys. Rev.* B **59** 12301
[21] Vanderbilt D 1990 *Phys. Rev.* B **41** 7892
[22] Perdew J P, Chevary J A, Vosko S H, Jackson K A, Pederson M R, Singh D J and Fiolhais C 1992 *Phys. Rev.* B **46** 6671
White J A and Bird D M 1994 *Phys. Rev.* B **50** 4954
[23] Kresse G and Furthmüller 1996 *J. Comput. Mater. Sci.* **6** 15
[24] Chadi D J and Cohen M L 1973 *Phys. Rev.* B **8** 5747
[25] Lide D R and Frederikse H P R 1997 *CRC Handbook of Chemistry and Physics* 78th edn (Boca Raton, FL: CRC press)
[26] Greeley J and Mavrikakis M 2003 *Surf. Sci.* **540** 215
[27] Talbot J, Tildesley D J and Steele W A 1984 *Mol. Phys.* **51** 1331
[28] Kuchta B and Etters R D 1988 *J. Chem. Phys.* **88** 2793
[29] Hansen F Y and Bruch L W 1995 *Phys. Rev.* B **51** 2515
[30] Leatherman G S and Diehl R D 1997 *Langmuir* **13** 7063
[31] Gruyters M and Jacobi K 1994 *Chem. Phys. Lett.* **225** 309
[32] Bruch L W 1983 *J. Chem. Phys.* **79** 3148
[33] Faßbender S, Enderle M, Knorr K, Noh J D and Rieger H 2002 *Phys. Rev.* B **65** 165411
[34] Da Silva J L F and Stampfl C 2007 *Phys. Rev.* B **76** 085301
[35] Bludau H, Gierer M, Over H and Ertl G 1994 *Chem. Phys. Lett.* **219** 352
[36] Yang S, Zhao G-L and Phillips J M 2008 private communication